Carbonylation of Dimethyl Ether with CO on Solid 12-Tungstophosphoric Acid: In Situ Magic Angle Spinning NMR Monitoring of the Reaction Kinetics

ARTICLE *in* THE JOURNAL OF PHYSICAL CHEMISTRY C · MAY 2013

Impact Factor: 4.77 · DOI: 10.1021/jp401604r

3 AUTHORS:

Maxim S Kazantsev
Novosibirsk Institute of Organic Chemistry
9 PUBLICATIONS **52** CITATIONS
SEE PROFILE

Mikhail V. Luzgin Dr
Boreskov Institute of Catalysis
49 PUBLICATIONS **772** CITATIONS
SEE PROFILE

Alexander G Stepanov
Boreskov Institute of Catalysis
136 PUBLICATIONS **1,681** CITATIONS
SEE PROFILE

THE JOURNAL OF PHYSICAL CHEMISTRY C

Article

pubs.acs.org/JPCC

Carbonylation of Dimethyl Ether with CO on Solid 12-Tungstophosphoric Acid: In Situ Magic Angle Spinning NMR Monitoring of the Reaction Kinetics

Maxim S. Kazantsev, Mikhail V. Luzgin, and Alexander G. Stepanov*

Boreskov Institute of Catalysis, Siberian Branch of Russian Academy of Sciences, Prospekt Akademika Lavrentieva 5, Novosibirsk 630090, Russia

ABSTRACT: Knowledge of the elementary steps of the reaction on the surface of a heterogeneous catalyst is crucial for understanding the reaction mechanism. This valuable information could be provided by in situ monitoring of the reaction with solid-state NMR spectroscopy. In this paper, the kinetics of the dimethyl ether (DME) carbonylation on 12-tungstophosphoric acid has been followed with high temperature ^{1}H magic angle spinning (MAS) NMR. The equilibrium of the initial ether activation toward the intermediate surface methoxy species has been examined with ^{13}C MAS NMR as well. The energy profile of DME carbonylation with CO to the Keggin acetate on $H_3PW_{12}O_{40}$ has been established. The apparent activation energy of the carbonylation, 95 ± 10 kJ mol^{-1}, represents a sum (within experimental error) of the standard enthalpy of the methoxy group formation, 57 ± 4 kJ mol^{-1}, and the activation barrier of the rate-determining step of the process, the interaction between methoxy group and carbon monoxide, 50 ± 4 kJ mol^{-1}.

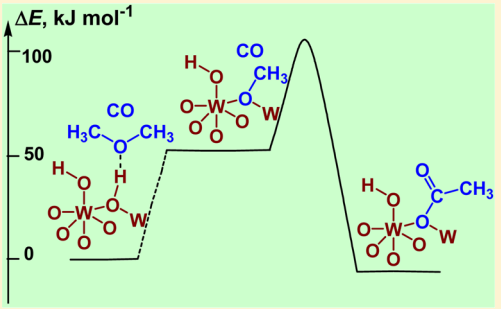

1. INTRODUCTION

Studies of the mechanisms of catalytic hydrocarbon conversion represent a significant challenge in terms of a goal-seeking search for new processes as well as improvement of the existing ones for hydrocarbon processing. This is the case for the carbonylation of methanol and dimethyl ether (DME) with carbon monoxide to produce acetic acid and methyl acetate. Indeed, the carbonylation of methanol using homogeneous iodine Rh and Ir complexes in the presence of iodide promoter[1−5] is the main method of acetic acid production at the industrial level. Taking into account the corrosive properties of iodide compounds, the development of a heterogeneous system which catalyzes this reaction in the absence of iodide additives is of great importance.[6]

It has been demonstrated recently that halide-free carbonylation of methanol and dimethyl ether could be realized on acid forms of zeolites (H−MOR, H−BEA, H−ZSM-5)[7,8] and on solid 12-tungstophosphoric acid (heteropolyacid, HPA) and its cesium salts,[9−11] with the reaction occurring with high selectivity and under considerably milder conditions in comparison with liquid acid catalysts.[12] These results have encouraged studies of the reaction mechanism using kinetic, IR, and desorption experiments,[8] NMR spectroscopy,[11,13−15] and theoretical methods.[16] Among all intermediates suggested for the carbonylation of methanol and DME, only the surface methoxy groups have been reliably identified for zeolite-catalyzed reaction.[13] As far as the carbonylation of DME and methanol on heteropolyacid catalyst is concerned, both the methoxy group[17,18] and the surface acetate, as well as the processes of their interconversion and transformation into target products, acetic acid or methyl acetate, have been monitored.[11,15]

Besides direct observation of the intermediates by spectroscopic methods, significant information on the reaction mechanisms can be obtained from kinetic studies. In particular, this is the case when one can monitor the kinetics of a certain elementary reaction stage. The kinetics data can serve as a base for the theoretical computations of probable reaction pathways, as well as to mark out the reactive intermediate species in the case when the activation of a single reagent results in formation of a set of intermediate species.

We have demonstrated recently that the surface methoxy group represents the main intermediate formed from methanol or dimethyl ether during their carbonylation with CO on solid 12-tungstophosphoric heteropolyacid, $H_3PW_{12}O_{40}$,[11] and its cesium salts.[15] In addition, the formation of trimethyloxonium ion in equilibrium with methanol (or DME) and methoxide has been observed. The insertion of carbon monoxide at the CH_3−O bond of methoxide occurs at considerably higher temperatures in comparison with that required for the methoxy group formation and further conversion of acetate fragment generated at this insertion. Therefore, we suppose the reaction of CO insertion to be a rate-determining stage of the carbonylation.[11,15] In addition, we have managed to prepare the methoxy group on the surface of $H_3PW_{12}O_{40}$ selectively, i.e., in the absence of other species.[11] This opens up further prospects to study this catalytic system including the measurement of the kinetics for elementary reaction steps.

Received: February 14, 2013
Revised: April 23, 2013
Published: April 23, 2013

dx.doi.org/10.1021/jp401604r | J. Phys. Chem. C 2013, 117, 11168−11175

In present paper we report on our studies of DME carbonylation on solid HPA by using high-temperature ^{1}H and ^{13}C magic angle spinning (MAS) NMR. ^{1}H MAS NMR allows in situ monitoring of the kinetics of both the entire reaction and the single stage of the interaction between the methoxy group and carbon monoxide. ^{13}C MAS NMR provides information on the equilibrium between the initial DME and the intermediate methoxy group formed from DME. The obtained values of activation barriers and the standard enthalpy of methoxide formation are well rationalized in terms of a quasi-equilibrium kinetic model.

2. EXPERIMENTAL SECTION

2.1. Materials. The sample of heteropolyacid (HPA), $H_3PW_{12}O_{40}\cdot 15H_2O$, was prepared according to the conventional procedure, including the synthesis of the sodium form, and the extraction of $H_3PW_{12}O_{40}$ with diethyl ether followed by recrystallization in water for purification. The BET surface area of this sample was 8 $m^2\ g^{-1}$. The concentration of acidic protons in anhydrous samples, measured from the ^{1}H MAS NMR spectrum using TMS as internal standard, was 1025 μmol g^{-1}, which is in good accordance with the chemical composition of HPA.

Methanol (of 99.0% purity), dimethyl ether (of 99.0% purity), carbon monoxide (of ≥99.0% purity), and dimethyl ether-$^{13}C_2$ (99 atom % ^{13}C), and carbon monoxide-^{13}C (99 atom % ^{13}C) were purchased from Aldrich Chemical Co. Inc. and were used without further purification.

2.2. Sample Preparation. The reaction was carried out in a sealed glass tube of 3.0 mm outer diameter and 10 mm length. This axially high symmetric sealed glass tube could be tightly inserted into a 4 mm o.d. zirconia rotor for subsequent in situ NMR analysis of the reaction intermediates and products. The samples of HPA (~80 mg) were calcined first in air by increasing the temperature from 300 to 523 K with a rate of 4 K min^{-1}. Further, the samples were maintained at 523 K for 5 h under vacuum with a residual pressure of less than 10^{-2} Pa.

The adsorption of methanol (ca. 200 μmol g^{-1}), DME (ca. 70 μmol g^{-1}), and carbon monoxide (90−170 μmol g^{-1}) on anhydrous HPA were performed at the temperature of liquid nitrogen. To selectively prepare the methoxy group on the HPA surface, the sample of HPA with methanol was held at 343 K for 1 h and then evacuated at this temperature for 1 h.[11]

The glass tubes with the samples containing the adsorbed reactants were sealed off from the vacuum system at the temperature of liquid nitrogen. Further, the samples were inserted into the rotors for in situ NMR analysis.

2.3. NMR Experiments. ^{1}H and ^{13}C MAS NMR spectra were recorded on a Bruker AVANCE-400 spectrometer (Larmor frequencies of 400 and 100.613 MHz, respectively) in the temperature range 293−493 K. For recording ^{1}H NMR spectra, a Hahn spin-echo pulse sequence (90−τ−180−τ−acquisition) was used, where τ was equal to the period of rotor spinning, 200 μs. The following conditions were used for recording the spectra: 4.9 μs length of 90° ^{1}H pulse; the delay time between scans was 3 s. For each ^{1}H MAS NMR spectrum, 20−40 scans were collected.

^{13}C MAS NMR spectra with high power proton decoupling were recorded with or without cross-polarization (CP) denoted below as ^{13}C CP/MAS NMR and ^{13}C MAS NMR. The following conditions were used for recording the spectra with CP: the proton high power decoupling field strength was 11.5 G (4.9 μs length of 90° ^{1}H pulse), the contact time was 4 ms at the Hartmann−Hahn matching condition of 50 kHz, and the delay time between scans was 3 s. The single pulse excitation ^{13}C MAS NMR spectra were recorded with a 90° flip angle, ^{13}C pulses of 4.9 μs duration, and 12 s recycle delay, which satisfies the $10T_1$ condition. High power proton decoupling in these experiments was used only during the acquisition time. A few thousand scans were collected for each ^{13}C CP/MAS NMR spectrum, and 40−640 scans were collected for each ^{13}C MAS NMR spectrum. The spinning rate was 5 kHz. ^{1}H and ^{13}C chemical shifts were referenced with respect to TMS as an external standard with an accuracy of ±0.5 ppm. The precision in the determination of the relative line position was 0.1−0.15 ppm.

The sample temperature was controlled by a Bruker BVT-2000 variable-temperature unit. The calibration of the temperature inside the rotor was performed with an accuracy of ±2 K by using lead nitrate as a ^{207}Pb MAS NMR chemical shift thermometer.[19]

3. RESULTS AND DISCUSSION

It has been shown recently that both solid 12-tungstophosphoric acid and its cesium salts catalyze carbonylation of methanol and dimethyl ether.[9−11,15] The main species formed from carbon monoxide and the alcohol on $H_3PW_{12}O_{40}$ (HPA) or the ether on $Cs_2HPW_{12}O_{40}$ were the acetate group bound to the Keggin anion (Keggin acetate) and acetic acid.[11,15] These species represented the precursors of the target product, methyl acetate (MA). The Keggin acetate and acetic acid convert readily to MA under interaction with excess DME.[15] Analysis of the kinetics of this reaction could provide more details on the mechanism of this reaction. The kinetics can be analyzed with solid-state NMR. With the use of high-temperature ^{1}H MAS NMR, one can follow in situ the kinetics of DME and the intermediate methoxy group transformation to the Keggin acetate and the final reaction product, MA. At the same time, ^{13}C MAS NMR can provide monitoring of the interconversion of DME and the intermediate methoxy species. Note, however, that the details of the interaction of the particular reaction of DME and CO interaction on $H_3PW_{12}O_{40}$ have not been reported yet. Therefore, we perform the analysis of DME and CO interaction on $H_3PW_{12}O_{40}$ and then analyze the kinetics of this reaction.

3.1. Interaction of Dimethyl Ether with Carbon Monoxide: Carbonylation Reaction. Figure 1 shows the ^{13}C CP/MAS NMR spectra recorded for the products formed from DME-$^{13}C_2$ and ^{13}CO at 423 K on $H_3PW_{12}O_{40}$ (HPA). For neat DME a typical pattern of the products is observed. Unreacted DME is observed as two signals at 63 and 67 ppm (Figure 1a). We have earlier attributed these resonances to DME adsorbed on different Brønsted acid sites of HPA, e.g., on terminal and bridged oxygen atoms of the Keggin anion.[15] However, the essential low-field shift of the signal at 67 ppm in comparison with that from DME in solution (59.7 ppm[20]) may be due to the formation of protonated dimethyl ether. Indeed, protonated DME exhibits a chemical shift of 68 ppm in superacid solution.[21] The resonance at 59 ppm (Figure 1a) is typical for the methoxy group formed at the Brønsted acid site of HPA,[11,15,18] whereas the signal at 81 ppm (Figure 1a) is characteristic for the trimethyloxonium cation (TMOC).[21] Thus, the conversion of dimethyl ether on $H_3PW_{12}O_{40}$ occurs according to Scheme 1, producing the methoxy group, protonated ether, and TMOC. Methanol, which should be formed during the DME-to-methoxide conversion (Scheme 1), is transformed further to the methoxy group.

dx.doi.org/10.1021/jp401604r | J. Phys. Chem. C 2013, 117, 11168−11175

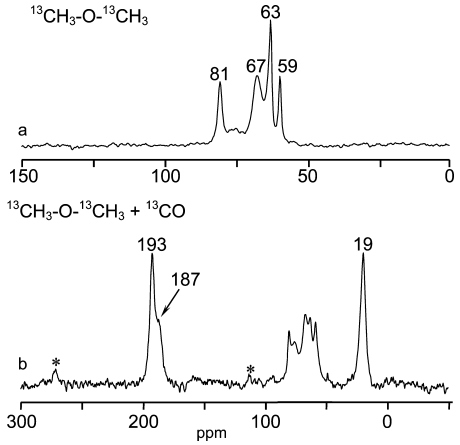

Figure 1. ^{13}C CP/MAS NMR spectra at 295 K of the products formed at 423 K on $H_3PW_{12}O_{40}$ from (a) DME-$^{13}C_2$ (30 min) and (b) DME-$^{13}C_2$ and ^{13}CO (3 h). Asterisks (∗) denote spinning sidebands.

Scheme 1. Conversion of Dimethyl Ether on Solid $H_3PW_{12}O_{40}$ at 293−423 K[a]

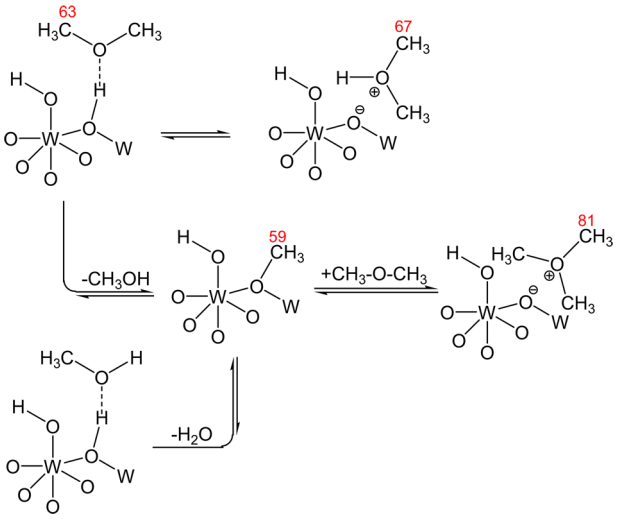

[a]Numbers in red correspond to peaks in Figure 1.

In the presence of a co-reactant, carbon monoxide, the same species are also observed at 59−81 ppm (Figure 1b). In addition, the resonances from the carbonylation products appear. Two signals in the carbonyl region of the spectrum, at 193 and 187 ppm, belong to the well-characterized acetate fragment bound to the Keggin anion (Keggin acetate) and acetic acid.[11,15] The resonances from the methyl groups of the Keggin acetate and acetic acid seem to be very close to each other and are not distinguished.[22] The signals from both methyl groups are observed at 19 ppm (Figure 1b). Thus, the carbonylation of DME on $H_3PW_{12}O_{40}$ proceeds analogously to that of methanol on this catalyst.[11,15] The observed Keggin acetate is the result of the CO insertion into the O−CH_3 bond of the methoxy group. The Keggin acetate is then partially hydrated into acetic acid (Scheme 2).

To gain a deeper insight into the peculiarities of the carbonylation, we have further analyzed the kinetics of the entire reaction, as well as the kinetics and thermodynamics of separate reaction stages, and tried to make correlations between these data.

3.2. Kinetics of DME Carbonylation on $H_3PW_{12}O_{40}$. The sensitivity of ^{13}C NMR spectroscopy does not allow deriving a

Scheme 2. Key Stage of Dimethyl Ether Carbonylation on $H_3PW_{12}O_{40}$: CO Insertion into the O−CH_3 Bond of the Methoxy Group[a]

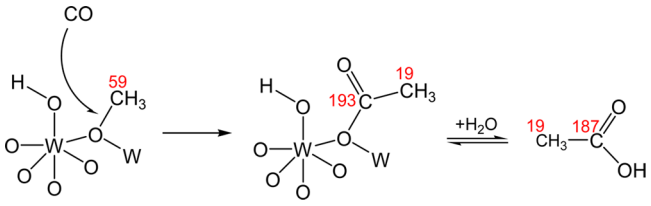

[a]Numbers in red correspond to peaks in Figure 1.

representative kinetics for the DME carbonylation reaction. Therefore, ^1H MAS NMR has been chosen for this purpose. Figure 2 shows the ^1H MAS NMR spectra of DME reacting with CO on $H_3PW_{12}O_{40}$ as a function of the reaction time.

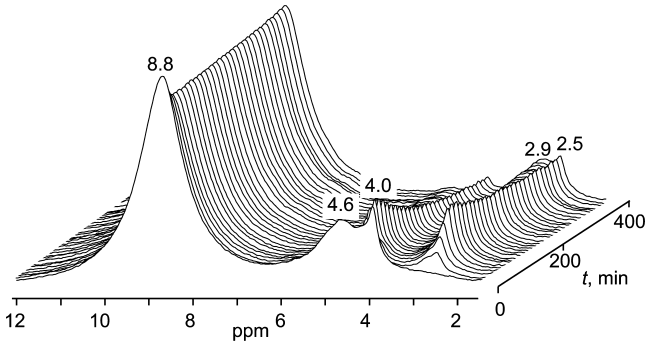

Figure 2. Stack plot of the ^1H MAS NMR spectra at 453 K of dimethyl ether adsorbed on $H_3PW_{12}O_{40}$ and reacting with carbon monoxide. The first spectrum (bottom) was recorded 5 min after the temperature was increased to 453 K, and the last spectrum (top) was recorded after 400 min of reaction duration. The time between subsequent spectra recordings was 12.7 min.

The decreasing signals at 4.6 and 4.0 ppm arise from the CH_3−O moiety.[23,24] The resonance at 4.0 ppm belongs to the adsorbed DME; the broad signal centered at 4.6 ppm is due to the mixture of the methoxy group, protonated ether, and TMOC[21,23−25] formed from the ether via rapidly equilibrated reactions of Scheme 1. The increasing resonances at ca. 2.9 and 2.5 ppm arise from the CH_3 groups of the Keggin acetate and acetic acid.[24] The signal from the acetic acid increases for 1 h to its maximum value and further its intensity almost does not change, while the intensity of the signal from the Keggin acetate increases evenly for the whole reaction time. This can be related to the fast interaction of water, evolved at DME to the methoxy group transformation, with the Keggin acetate until the quantity of water evolved is completely exhausted. For obtaining the kinetic curve, we have used the total intensity of the signals at 2.9 and 2.5 ppm from the Keggin acetate and acetic acid.

Figure 3 shows experimental and simulated kinetics of the DME carbonylation. The experimental points were fitted using a simple function of exponential growth:

$$C_{\text{acetate+AcOH}} = C_0(1 - e^{-kt}) \quad (1)$$

where $C_{\text{acetate+AcOH}}$ is the current concentration and C_0 is the final concentration of the Keggin acetate and acetic acid; k is the effective rate constant. Simulation of experimental kinetics curves offers values of the effective rate constant k for the DME

dx.doi.org/10.1021/jp401604r | J. Phys. Chem. C 2013, 117, 11168−11175

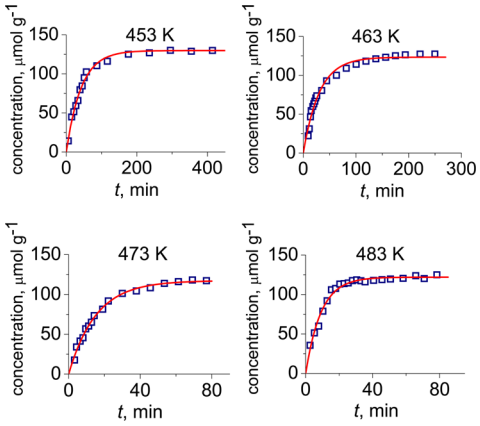

Figure 3. Experimental and simulated (solid curves) kinetics of dimethyl ether carbonylation on $H_3PW_{12}O_{40}$.

carbonylation and its initial rate $W^0_{DME} = kC_0$ at different reaction temperatures (Table 1). Since the reaction is complex and includes the formation of the intermediate species, the temperature dependence of the initial reaction rate, W^0_{DME}, was used for the determination of the activation energy. The Arrhenius plot for W^0_{DME} (Figure 4) gives an activation energy of 95 kJ mol^{-1}, which exceeds the values of 55−75 kJ mol^{-1} estimated from ref 8 for the DME carbonylation on acidic zeolites.

As we have earlier established, the methoxy group as the intermediate of the carbonylation of DME or methanol can be generated as the sole species on the surface of $H_3PW_{12}O_{40}$ from methanol.[11] The methoxy group transforms directly to the Keggin acetate and further to the acetic acid as shown by ^{13}C MAS NMR.[11] The interaction between the methoxy group and carbon monoxide seems to be the elementary stage of the DME carbonylation reaction. The kinetics of this stage could be monitored with NMR.

Figure 5 shows the evolution of ^1H MAS NMR spectra of the methoxy group (generated from methanol; see the Experimental Section) during the reaction with carbon monoxide on $H_3PW_{12}O_{40}$ at 453 K. The methoxy group is observed at 4.3 ppm and gradually transforms into the Keggin acetate with the signal at 2.9 ppm.

Table 1. Initial Rates of the DME Carbonylation (W^0_{DME}), Rate Constants of the Reaction between Methoxy Group and CO (k_{MeO}), Equilibrium Constants (K^{eq}_{MeO}) of DME to the Methoxy Group Formation on $H_3PW_{12}O_{40}$, and the Product of k_{MeO} and Initial Quasi-Equilibrium Concentration of Methoxy Group (k_{MeO}[MeO])

T, K	W^0_{DME}, μmol g^{-1} min^{-1}	k_{MeO}, g μmol^{-1} min^{-1}	K^{eq}_{MeO}	k_{MeO}[MeO], min^{-1}
403			$(8.7 \pm 0.6) \times 10^{-3}$	
413			$(1.3 \pm 0.1) \times 10^{-2}$	
423			$(2.1 \pm 0.2) \times 10^{-2}$	
433			$(2.7 \pm 0.2) \times 10^{-2}$	
453	3.1 ± 0.2	$(0.9 \pm 0.05) \times 10^{-4}$		$(5.1 \pm 0.3) \times 10^{-3}$
463	4.1 ± 0.4	$(1.4 \pm 0.08) \times 10^{-4}$		$(9.5 \pm 0.5) \times 10^{-3}$
473	7.6 ± 0.5	$(2.0 \pm 0.1) \times 10^{-4}$		$(16 \pm 0.8) \times 10^{-3}$
483		$(2.7 \pm 0.1) \times 10^{-4}$		$(25.1 \pm 0.9) \times 10^{-3}$
493	13.9 ± 1.1			

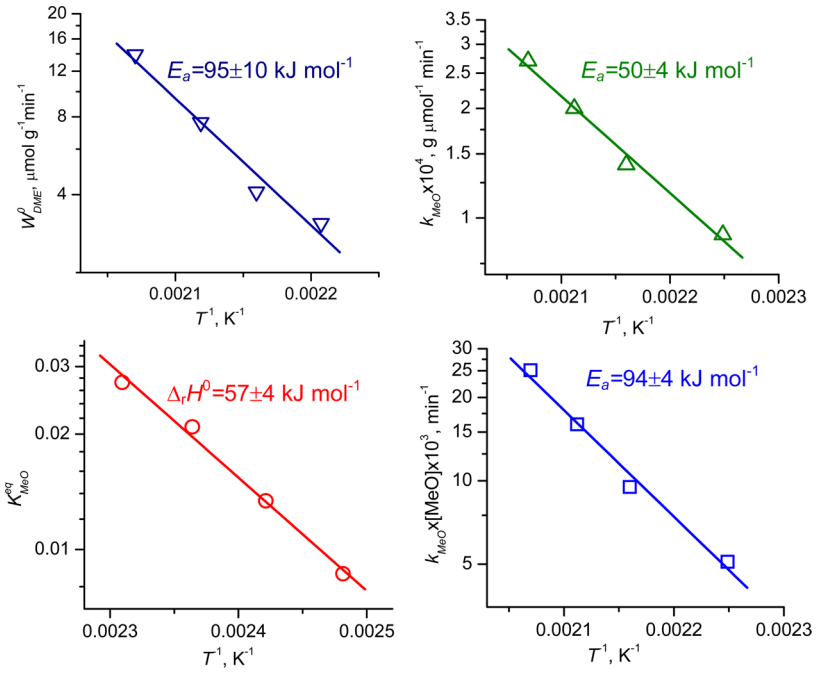

Figure 4. Arrhenius plots for the initial rate, W^0_{DME}, of the dimethyl ether carbonylation (▽) and for the rate constant, k_{MeO}, of the reaction of methoxy group with carbon monoxide (△). Temperature dependences of the equilibrium constant K^{eq}_{MeO} for DME to methoxy group transformation on $H_3PW_{12}O_{40}$ (○) and of the product of k_{MeO} and initial quasi-equilibrium concentration of methoxy groups, k_{MeO}[MeO] (□).

dx.doi.org/10.1021/jp401604r | J. Phys. Chem. C 2013, 117, 11168−11175

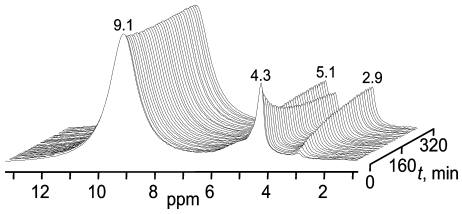

Figure 5. Stack plot of the ^{1}H MAS NMR spectra at 453 K of the methoxy group on $H_3PW_{12}O_{40}$ reacting with carbon monoxide. The first spectrum (bottom) was recorded 5 min after the temperature was increased to 453 K, and the last spectrum (top) was recorded after 320 min of reaction duration. The time between subsequent spectra recordings was 9 min.

The carbonylation process is accompanied by the growth of the signal at 5.1 ppm. Note that the total intensity of the signals from the methoxy and acetate protons is unchanged during the reaction and is equal to the initial intensity of the methoxy group resonance. Therefore, the signal at 5.1 ppm cannot arise from any reaction intermediate or the product. A similar chemical shift has been reported for the OH groups of $H_3PW_{12}O_{40}$ dispersed on various supports.[26,27] This line is upfield shifted in comparison with the resonance typical for bulk HPA, ca. 9 ppm (see Figures 2 and 5).[26−28] The appearance of the 5.1 ppm signal for HPA on various supports was rationalized by the lack of hydrogen bonds of this OH group with the neighboring Keggin units, which usually exist in the bulk of the HPA structure.[29] Hence, the line at 5.1 ppm is attributed to the OH groups of the Keggin anions that do not interact with the neighboring anions by hydrogen bonding. For example, these OH groups could be located on the outer surface of the Keggin anion.[26,27] Alternatively, they are located in the internal void of the secondary structure of HPA, but the distance between the neighboring anions for some reason is large enough for the OH group to form a hydrogen bond with the vicinal Keggin anion. Thus, we suppose that the formation of the Keggin acetate and/or acetic acid disrupts in part the hydrogen bonding among the Keggin anions in the secondary structure of HPA, resulting in the appearance of the signal at 5.1 ppm.

It should be also noted that according to literature data DME and methanol are adsorbed in the bulk of HPA.[30] Therefore, methoxy groups can be formed both at the surface and in the bulk of $H_3PW_{12}O_{40}$. In our experiments the concentration of methoxy groups is 100−140 μmol g^{-1}. At the same time, the concentration of surface OH groups, estimated based on the BET surface area of our sample (8 m^2 g^{-1}) and the surface area of the hemisphere of each Keggin unit (1.9 nm^2),[31] does not exceed 20 μmol g^{-1}. This indicates that methoxy groups are in fact formed at both the bulk and the surface Brønsted acid sites. Both types of methoxides are available for the interaction with CO since we observe their quantitative consumption by carbon monoxide. This observation contradicts at first glance the earlier conclusion that CO reveals reactivity only at the surface of HPA.[32] That conclusion was based on peculiarities observed for the oxidation of carbon monoxide on $H_3PMo_{12}O_{40}$. However, those data may reflect less reactivity of bulk Mo−O groups in comparison with surface ones toward CO oxidation rather than the inability of CO to penetrate the bulk of HPA. In addition, the situation with tungsten HPA may be different. Therefore, in the case of DME carbonylation on $H_3PW_{12}O_{40}$ we observe the reactivity of carbon monoxide on the surface and in the bulk of HPA.

Figure 6 shows experimental and simulated kinetics of the interaction of the methoxy group with carbon monoxide.

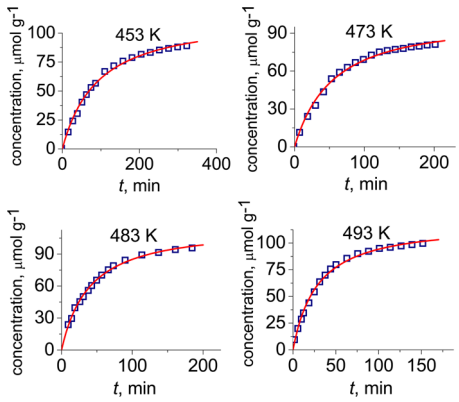

Figure 6. Experimental and simulated (solid curves) kinetics of the reaction of methoxy group with carbon monoxide on $H_3PW_{12}O_{40}$. Simulation was performed in accordance with the second-order irreversible kinetic scheme. The rate constants, k_{MeO}, which correspond to the solid curves, are given in Table 1.

According to our previous results, this reaction is irreversible.[11] Experimental points were fitted using a simple second-order kinetic model, in which the growth of the product concentration should satisfy the following equation:

$$C_{\text{acetate+AcOH}} = \frac{A^0(1 - e^{(B^0 - A^0)kt})}{(A^0/B^0) - e^{(B^0 - A^0)kt}} \quad (2)$$

where A^0 is the initial concentration of carbon monoxide (90−110 μmol g^{-1}) and B^0 is the initial concentration of methoxy groups (140 μmol g^{-1}).

The rate constants for the methoxy group carbonylation, k_{MeO}, obtained by the simulation of experimental kinetic curves on the basis of eq 2, are presented in Table 1. The Arrhenius plot for k_{MeO} (Figure 4) gives the activation energy E_{MeO} = 50 kJ mol^{-1}. This activation barrier for the elementary reaction step can hardly be compared with any data obtained earlier. Indeed, until now only theoretical studies of the elementary step of the kinetics of the DME carbonylation have been reported, and only for zeolite-catalyzed carbonylation. The value of the activation energy, estimated for the reaction between CO and the methoxy group on zeolite MOR,[16] is 2 times greater than the activation barrier obtained in the present study.

The apparent activation energy measured for the DME carbonylation, 95 kJ mol^{-1}, sufficiently exceeds that for the elementary stage of the CO interaction with surface methoxy group. This may be due to influence of the reaction stage, which precedes the stage of the methoxy group and CO interaction on the reaction energy profile. The preceding stage is the interaction of DME with the Keggin anion to form the methoxy group. This interaction is fast enough at the temperature of the carbonylation reaction so that the kinetics of this process cannot be followed with our experimental techniques. However, the equilibrium established between DME and the methoxy group on $H_3PW_{12}O_{40}$ can be analyzed by ^{13}C MAS NMR.

3.3. Monitoring the Equilibrium of DME to Methoxy Group Transformation. Figure 7 shows the evolution of ^{13}C MAS NMR spectra of DME-$^{13}C_2$ adsorbed on $H_3PW_{12}O_{40}$ as a function of the temperature. The temperature range chosen for equilibrium analysis, 403−433 K, differs from that used for the

dx.doi.org/10.1021/jp401604r | J. Phys. Chem. C 2013, 117, 11168−11175

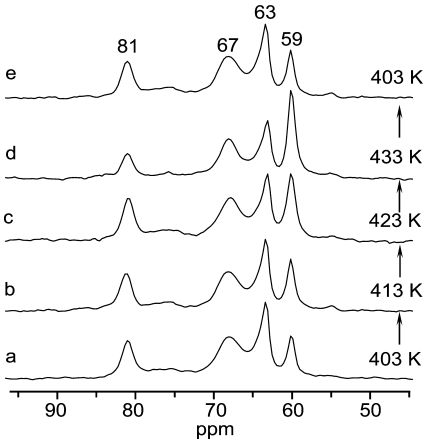

Figure 7. ^{13}C MAS NMR spectra recorded at 403−433 K for DME-$^{13}C_2$ adsorbed on $H_3PW_{12}O_{40}$.

carbonylation reaction performance since at higher temperature the secondary process of DME-to-hydrocarbon conversion occurs in the absence of carbon monoxide. The pattern of the reaction products, methoxy group (59 ppm), protonated dimethyl ether (67 ppm), and trimethyloxonium cation (81 ppm), does not vary from that observed in the room temperature spectrum (cf. Figures 1a and 7). The relative intensity of the signal from the methoxy group increases notably with increasing temperature, whereas the signal intensities of the other species do not change pronouncedly with temperature increase. The reverse decrease of the temperature from 433 to 403 K completely restores the pattern of the signal intensities (cf. Figure 7a and 7e). Thus, all the processes of Scheme 1 are in fact reversible and equilibrated.

It should be emphasized that the time required for the temperature equilibration and registration of a representative ^{13}C NMR spectrum with satisfactory signal-to-noise ratio, ca. 10 min, proved to be enough for the process equilibration even at the lowest temperature used. Further keeping the sample at each given temperature produces no alteration in the signal intensities. Thus, 10 min represents the upper limit for the characteristic time of all processes of DME conversion, including formation of the methoxy group, protonated ether, and trimethyloxonium cation. At the same time, the half-time for the reaction between the methoxy group and CO at 453 K is ca. 70 min. Using the activation energy of this reaction, the characteristic time can be estimated for the temperature range 403−433 K. This value should be in the range 120−360 min, which significantly exceeds the upper limit for the characteristic time of the equilibria depicted in Scheme 1. Therefore, we suppose that the carbonylation can be considered as a quasi-equilibrated process. The stages of the formation of the methoxy group, TMOC, and protonated ether are rapid and equilibrated, whereas the interaction of the methoxy group with carbon monoxide represents the rate-determining step of the reaction.

For the DME carbonylation on acidic zeolites, a quasi-equilibrium scheme has been also proposed.[8] The reaction of CO with the methyl group to form the surface acetyl intermediate is considered as the kinetically relevant step of the process. The equation derived for the stationary reaction rate correlated well with the kinetic experiments. In our case, for the reaction in the static reactor, the quasi-equilibrium approach implies that the reaction rate is proportional to the quasi-equilibrium concentration of the methoxy group: $W_{DME} \sim k_{MeO}[MeO]$. The latter concentration should be in turn roughly proportional to an equilibrium constant of the methoxy group formation from DME, K^{eq}_{MeO}, via the reaction

$$1/2\ CH_3{-}O{-}CH_3 + H{-}O{-}W\sim \overset{K^{eq}_{MeO}}{\rightleftharpoons} CH_3{-}O{-}W\sim + 1/2\ H_2O \qquad (3)$$

Therefore, $W_{DME} \sim k_{MeO}K^{eq}_{MeO}$. In this case, the apparent activation energy of the DME carbonylation is approximately equal to the sum of E_{MeO} and the enthalpy of the methoxy group formation from DME. K^{eq}_{MeO} can be defined on the basis of eq 3 using the following expression:

$$K^{eq}_{MeO} = \frac{[CH_3{-}O{-}W][H_2O]^{1/2}}{[CH_3OCH_3]^{1/2}[HO{-}W{-}]}$$

The equilibrium concentrations of DME and the methoxy groups are estimated from the ^{13}C MAS NMR spectra of Figure 7. The amount of evolved water is calculated on the basis of the stoichiometry of the reactions of Scheme 1. The equilibrium concentration of OH groups is estimated taking into account their consumption according to Scheme 1. The calculated values of the equilibrium constant are presented in Table 1. The plot of ln K^{eq}_{MeO} vs inverse temperature (Figure 4) gives the enthalpy of the reaction of the methoxy group formation from DME on $H_3PW_{12}O_{40}$: Δ_rH° = +57 kJ mol^{-1}. The theoretical studies of the methoxy group formation from methanol and DME on acidic zeolites showed also the endothermic character of this reaction.[16] The sum of E_{MeO} and Δ_rH° is equal to 107 kJ mol^{-1}, which is comparable (within experimental error) with the activation

Scheme 3. Energy Diagram of DME Carbonylation with CO to the Keggin Acetate on $H_3PW_{12}O_{40}$

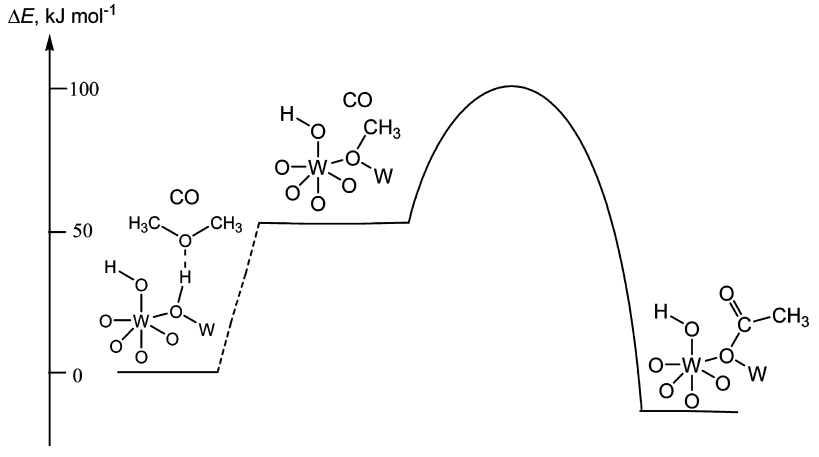

dx.doi.org/10.1021/jp401604r | J. Phys. Chem. C 2013, 117, 11168−11175

energy of the DME carbonylation: 95 kJ mol^{-1}. Thus the energy profile of DME carbonylation with CO to the Keggin acetate on $H_3PW_{12}O_{40}$ is established (Scheme 3).

To make a more accurate correlation between the parameters of separate stages and those of the overall reaction, we have taken into account all the rest of the equilibria depicted in Scheme 1 (see eqs 4 and 5), excluding that between methanol and methoxy group, since the concentration of the alcohol is negligible:

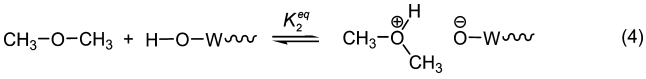

(4)

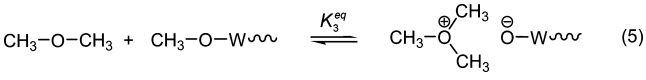

(5)

The temperature dependences of the equilibrium constants K^{eq}_{MeO}, K^{eq}_2, and K^{eq}_3 have allowed us to estimate the initial quasi-equilibrium concentrations of methoxy groups, [MeO], in the temperature range used for the carbonylation reaction. Using the obtained values of methoxy group concentration, the temperature dependence of the product k_{MeO}[MeO] has been evaluated (see Table 1). Since $W_{DME} \sim k_{MeO}$[MeO], one can expect that the activation energy derived from the temperature dependence of k_{MeO}[MeO] will better correlate with the apparent activation energy of the DME carbonylation. In fact, the obtained value, 96 ± 4 kJ mol^{-1} (Figure 4), is close to E_{DME}.

The observed correlation between the activation barrier of the elementary stage and that of the reaction as a whole confirms the hypothesis concerning the quasi-equilibrium model of the DME carbonylation on $H_3PW_{12}O_{40}$ under conditions used in our experiments. These results provide further evidence for the reaction between the methoxy group and carbon monoxide to be the key step of the DME carbonylation. The data obtained offer further opportunities for a complete description of the HPA-based catalytic systems for carbonylation of alcohols and ethers.

4. CONCLUSION

^{1}H and ^{13}C magic angle spinning (MAS) NMR spectroscopy has been used to analyze the elementary stages of the reaction of dimethyl ether (DME) carbonylation on solid 12-tungstophosphoric acid ($H_3PW_{12}O_{40}$). Using high-temperature ^{1}H MAS NMR in situ, the kinetics of the DME carbonylation reaction and in particular the elementary stage of the methoxy group interaction with CO have been analyzed. The equilibrium of the initial ether activation toward the intermediate surface methoxy species has been examined with ^{13}C MAS NMR as well. This allowed us to establish the energy profile of the reaction of DME carbonylation with CO to the Keggin acetate on $H_3PW_{12}O_{40}$. The apparent activation energy of the carbonylation reaction, 95 ± 10 kJ mol^{-1}, represents a sum (within experimental error) of the standard enthalpy of the methoxy group formation, 57 ± 4 kJ mol^{-1}, and the activation barrier of the rate-determining step of the process, the interaction between the methoxy group and carbon monoxide, 50 ± 4 kJ mol^{-1}. The obtained kinetic and thermodynamic parameters of the reaction offer opportunities for a complete description of the HPA-based catalytic systems for the reaction of carbonylation of alcohols and ethers.

AUTHOR INFORMATION

Corresponding Author

*Tel.: +7 952 905 9559. Fax: +7 383 3308056. E-mail: stepanov@catalysis.ru.

Notes

The authors declare no competing financial interest.

REFERENCES

(1) Paulik, F. E.; Roth, J. F. Novel Catalysts for Low-Pressure Carbonylation of Methanol to Acetic Acid. *Chem. Commun.* **1968**, 1578.

(2) Roth, J. F.; Craddock, J. H.; Hershman, A.; Roth, F. E. Low Pressure Process for Acetic Acid via Carbonylation of Methanol. *CHEMTECH* **1971**, *1*, 600−605.

(3) Schultz, R. G.; Montgomery, P. D. Vapor Phase Carbonylation of Methanol to Acetic Acid. *J. Catal.* **1969**, *13*, 105−106.

(4) Shultz, R. G. (Monsanto Co.). U.S. Patent 3,717,670, 1973.

(5) Howard, M. J.; Jones, M. D.; Roberts, M. S.; Taylor, S. A. C_1 to Acetyls: Catalysis and Process. *Catal. Today* **1993**, *18*, 325−354.

(6) Stepanov, A. G. Carbonylation—Heterogeneous. In *Encyclopedia of Catalysis*; Horvath, I. T., Ed.; Wiley-Interscience: New York, 2003; Vol. 2, pp 71−104.

(7) Ellis, B.; Howard, M. J.; Joyner, R. W.; Reddy, K. N.; Padley, M. B.; Smith, W. J. Heterogeneous Catalysts for the Direct, Halide-Free Carbonylation of Methanol. *Stud. Surf. Sci. Catal.* **1996**, *101*, 771−779.

(8) Cheung, P.; Bhan, A.; Sunley, G. J.; Law, D. J.; Iglesia, E. Site Requirements and Elementary Steps in Dimethyl Ether Carbonylation Catalyzed by Acidic Zeolites. *J. Catal.* **2007**, *245*, 110−123.

(9) Volkova, G. G.; Plyasova, L. M.; Salanov, A. N.; Kustova, G. N.; Yurieva, T. M.; Likholobov, V. A. Heterogeneous Catalysts for Halide-Free Carbonylation of Dimethyl Ether. *Catal. Lett.* **2002**, *80*, 175−179.

(10) Volkova, G. G.; Plyasova, L. M.; Shkuratova, L. N.; Budneva, A. A.; Paukshtis, E. A.; Timofeeva, M. N.; Likholobov, V. A. Solid Superacids for Halide-Free Carbonylation of Dimethyl Ether to Methyl Acetate. *Stud. Surf. Sci. Catal.* **2004**, *147*, 403−408.

(11) Luzgin, M. V.; Kazantsev, M. S.; Wang, W.; Stepanov, A. G. Reactivity of Methoxy Species toward CO on Keggin 12-$H_3PW_{12}O_{40}$: A Study with Solid State NMR. *J. Phys. Chem. C* **2009**, *113*, 19639−19644.

(12) Colquhoun, V. H. M.; Thompson, D. J.; Twigg, M. V. *Carbonylation: Direct Synthesis of Carbonyl Compounds*; Plenum Press: New York, 1991.

(13) Jiang, Y.; Hunger, M.; Wang, W. On the Reactivity of Surface Methoxy Species in Acidic Zeolites. *J. Am. Chem. Soc.* **2006**, *128*, 11679−11692.

(14) Bhan, A.; Allian, A. D.; Sunley, G. J.; Law, D. J.; Iglesia, E. Specificity of Sites within Eight-Membered Ring Zeolite Channels for Carbonylation of Methyls to Acetyls. *J. Am. Chem. Soc.* **2007**, *129*, 4919−4924.

(15) Luzgin, M. V.; Kazantsev, M. S.; Volkova, G. G.; Wang, W.; Stepanov, A. G. Carbonylation of Dimethyl Ether on Solid Rh-Promoted Cs-Salt of Keggin 12-$H_3PW_{12}O_{40}$: A Solid-State NMR Study of the Reaction Mechanism. *J. Catal.* **2011**, *277*, 72−79.

(16) Boronat, M.; Martinez-Sanchez, C.; Law, D.; Corma, A. Enzyme-like Specificity in Zeolites: A Unique Site Position in Mordenite for Selective Carbonylation of Methanol and Dimethyl Ether with CO. *J. Am. Chem. Soc.* **2008**, *130*, 16316−16323.

(17) Farneth, W. E.; Staley, R. H.; Domaille, P. J.; Farlee, R. D. Comparison of Structure and Thermal Chemistry of Stoichiometric and Catalytic Alkoxy-Substituted Molybdenum Heteropolyanions: ^{13}C CP-MAS NMR Spectrum of a Chemisorbed Reaction Intermediate. *J. Am. Chem. Soc.* **1987**, *109*, 4018−4023.

(18) Zhang, H. L.; Zheng, A. M.; Yu, H. G.; Li, S. H.; Lu, X.; Deng, F. Formation, Location, and Photocatalytic Reactivity of Methoxy Species on Keggin 12-$H_3PW_{12}O_{40}$: A Joint Solid-State NMR Spectroscopy and DFT Calculation Study. *J. Phys. Chem. C* **2008**, *112*, 15765−15770.

(19) Ferguson, D. B.; Haw, J. F. Transient Methods For in situ NMR of Reactions on Solid Catalysts Using Temperature Jumps. *Anal. Chem.* **1995**, *67*, 3342−3348.

(20) Roberts, J. D.; Christl, M.; Reich, H. J. Nuclear Magnetic Resonance Spectroscopy. Carbon-13 Chemical Shifts of Methycyclo-

pentanes, Cyclopentanols, and Cyclopentyl Acetates. *J. Am. Chem. Soc.* **1971**, *93*, 3463−3468.
(21) Olah, G. A.; Doggweiler, H.; Felberg, J. D.; Fronlich, S. Onium Ions. *J. Org. Chem.* **1985**, *50*, 4847−4851.
(22) Kazantsev, M. S.; Luzgin, M. V.; Volkova, G. G.; Stepanov, A. G. Carbonylation of Dimethyl Ether on $Rh/Cs_2HPW_{12}O_{40}$: Solid-State NMR Study of the Mechanism of Reaction in the Presence of a Methyl Iodide Promoter. *J. Catal.* **2012**, *291*, 9−16.
(23) Lacey, M. J.; Macdonald, C. G.; Pross, A.; Shannon, J. S.; Sternhell, S. Geminal Interproton Coupling Constants in Some Methyl Derivatives. *Aust. J. Chem.* **1970**, *23*, 1421−1429.
(24) Gottlieb, H. E.; Kotlyar, V.; Nudelman, A. NMR Chemical Shifts of Common Laboratory Solvents as Trace Impurities. *J. Org. Chem.* **1997**, *62*, 7512−7515.
(25) Olah, G. A.; O'Brien, D. H. Stable Carbonium Ions. XXXVI.[1a] Protonated Aliphatic Ethers and Their Cleavage to Carbonium Ions. *J. Am. Chem. Soc.* **1967**, *89*, 1725−1728.
(26) Mastikhin, V. M.; Kulikov, S. M.; Nosov, A. V.; Kozhevnikov, I. V.; Mudrakovskii, I. L.; Timofeeva, M. N. ^{1}H and ^{31}P MAS NMR Studies of Solid Heteropolyacids and $H_3PW_{12}O_{40}$ Supported on SiO_2. *J. Mol. Catal.* **1990**, *60*, 65−70.
(27) Mastikhin, V. M.; Terskikh, V. V.; Timofeeva, M. N.; Krivoruchko, O. P. ^{1}H, ^{31}P NMR MAS, Infrared and Catalytic Studies of Heteropolyacid $H_3PW_{12}O_{40}$ Supported on MgF_2. *J. Mol. Catal. A* **1995**, *95*, 135−140.
(28) Kanda, Y.; Lee, K. Y.; Nakata, S.; Asaoka, S.; Misono, M. Solid-State NMR of $H_3PW_{12}O_{40}\cdot nH_2O$ and $H_3PW_{12}O_{40}\cdot 6C_2H_5OH$. *Chem. Lett.* **1988**, 139−142.
(29) Misono, M.; Sakata, K.; Yoneda, Y.; Lee, W. Y. Acid-Redox Bifunctional Properties of Heteropoly Compounds of Molybdenum and Tungsten Correlated with Catalytic Activity for Oxidation of Methacrolein. *Stud. Surf. Sci. Catal.* **1981**, *7*, 1047−1059.
(30) Okuhara, T.; Mizuno, N.; Misono, M. Catalytic Chemistry of Heteropoly Compounds. *Adv. Catal.* **1996**, *41*, 113−252.
(31) Ma, Z.; Hua, W.; Ren, Y.; He, H.; Gao, Z. n-Butane Isomerization over Cs-Salt of $H_3PW_{12}O_{40}$: A Mechanistic Study by ^{13}C MAS NMR. *Appl. Catal., A* **2003**, *256*, 243−250.
(32) Mizuno, N.; Watanabe, T.; Misono, M. Catalysis by Heteropoly Compounds. VIII. Reduction-Oxidation and Catalytic Properties of 12-Molybdophosphoric Acid and Its Alkali Salts. The Role of Redox Carriers in the Bulk. *J. Phys. Chem.* **1985**, *89*, 80−85.